PERGAMON

International Journal of Heat and Mass Transfer 43 (2000) 3883–3895

International Journal of HEAT and MASS TRANSFER

www.elsevier.com/locate/ijhmt

# Axisymmetric transient solutions of the heat diffusion problem in layered composite media

M.F. Abdul Azeez*, A.F. Vakakis

*Department of Mechanical and Industrial Engineering, University of Illinois at Urbana-Champaign, Urbana, IL 61801, USA*

**Abstract**

An analytical/numerical method for solving the problem of non-stationary heat diffusion in multilayered slabs is presented. This is an extension of previous methods that have been used to solve transient heat diffusion problems in one-dimension. In this work, two-dimensional semi-infinite media are considered and double integral transforms are used to obtain the corresponding transfer matrix form from the governing partial differential equations. Numerical techniques are used to compute the overall transfer matrices of the system and to numerically invert them in order to obtain transient results. Difficulties encountered with the numerical operations and ways to circumvent these are presented. The developed methodology has been applied to two-layered configurations. 

## 1. Introduction

Heat conduction in composite media has been the topic of intensive research in recent years. A theoretical understanding of the problem of heat conduction in composite media is of importance in diverse fields, such as oil shale retorting, reinforced laminates, hydrodynamics of stratified fluids and protective coating of turbine blades, to name a few. Transient heat conduction has been dealt with in several ways. Baker-Jarvis et al. [1] used the Greens function technique to analytically obtain the transient temperatures in a one-dimensional composite medium. Of course, a host of numerical methods based on the finite difference and finite element schemes are also available. The governing partial differential equation for transient heat conduction is essentially parabolic in nature. In [2,3], a hyperbolic equation is considered to solve the heat conduction problem. The problem is treated as a wave propagation problem with heavy damping. This technique has been applied to transient conduction in semi-infinite media. However, the application of this technique to composite media is limited. In [4], Yalamanchili and Chu provide a method wherein the use of a variational approach bordering on the Finite Element Method is used to model heat transfer in composite media. This method also provides approximate solutions for non-linear boundary conditions of the linear problem. In [5], the transient two-dimensional conductive and radiative heat transfer problem is analyzed. But the work that is of relevance to the present exposition is that of Bouzidi and Duhamel [6], where the eigenvalue problem associated with thermal diffusion problem is solved.

* Corresponding author. Present address: GE Corporate R&D Center, Bldg K-1, Rm 4B36, One Research Circle, Niskayuna, NY 12309, USA. Tel.: +1-518-387-4212; fax: +1-518-387-7292.

*E-mail address:* mohammed@crdns.crd.ge.com (M.F.A. Azeez).

0017-9310/00/$ - see front matter 
PII: S0017-9310(99)00386-5

**Nomenclature**

| | |
|---|---|
| $[C]$ | direct global stiffness matrix |
| $F$ | flux in the scaled coordinate system |
| $H$ | thickness of the layer |
| $N$ | number of bi-periodic layers in the system |
| $T$ | temperature in the scaled and unscaled coordinate system |
| $[T_{set}]$ | transfer matrix relating states in the top and bottom layers |
| $f$ | flux in the unscaled coordinate system |
| $h$ | depth inside the layer where the states are to be computed |
| $(r, z)$ | unscaled coordinate system |
| $s$ | Laplace transform variable |
| $t$ | time |
| *Greek symbols* | |
| $\alpha$ | diffusivity of the medium |
| $[\alpha]$ | matrix $[T_{set}]^N$ |
| $\eta$ | scattering constant |
| $\mu$ | Hankel transform variable |
| $\omega$ | non-dimensional frequency |
| $\rho C_p$ | heat capacity |
| $(\rho, \zeta)$ | scaled coordinate system |
| $\tau$ | scaled time |
| $\tau^*$ | thermal impedance |

The concept of transfer matrix has been used in that work, in conjunction with finite integral transforms to analyze transient heat conduction in a one-dimensional composite layered system.

In the work presented here, transient heat conduction of a semi-infinite composite media has been investigated. The medium is axisymmetric in nature and the problem can be reduced to two dimensions. Double integral transforms (Fourier and Hankel transforms) are employed to reduce the governing partial differential equations (PDEs) to a set of ordinary differential equations (ODEs). The double integral transform technique used here has parallels that are used by Cetinkaya and coworkers [7–11] in the wave propagation context. In these works, double integral transforms were employed to analyze transient stress wave propagation in sets of bi-layered medium composed of materials with different mechanical impedance properties.

The governing PDE for a single slab is first considered. This equation is non-dimensionalized and then double integral transforms are used to convert the PDEs into a system of ODEs. Then the boundary conditions are applied and a transfer matrix relating the flux and temperatures on both surfaces of the slab is derived. Using this transfer matrix for the individual slabs, the transfer matrix for the structure consisting of many slabs is assembled, and the temperatures and fluxes at any desired location can be obtained after a double inversion of the corresponding transformed quantities. A numerical scheme based on the Direct Global Transfer Method which avoids the problem of exponential dichotomy [11] is presented. Numerical simulations have been performed on two different systems to study transient temperature distributions in layered media.

It was pointed out by a reviewer that the work on integral transform techniques applied to heat transfer problems was reported first in [12]. The theory behind the application of integral transformations is postulated in great depth in the book by Ozisik [13] where several different transformations are given depending on the situation. Some numerical aspects are discussed in [12], however, there are far severe numerical instabilities that arise when the number of layers is unlimited and we address those issues in this paper. The comments of the reviewer is acknowledged.

## 2. Formulation

### 2.1. Definitions

A *layer* is defined here as a plate that is homogeneous and isotropic and that has finite thickness, but extends to infinity in the other two dimensions. It is hence convenient to express the governing equations in cylindrical coordinate system. A *bi-periodic* set is a structure in which two layers of different thermal and geometric properties are brought together in perfect mechanical contact. Each bi-periodic set may be composed of strongly and weakly conducting layers, which shall be referred to as Layer A and Layer B, respectively. A *system* considered here consists of $N$ bi-periodic sets, again, with perfect bonding between them. The number of layers in a system can be unlimited. An *interface* is a plane where, either two bi-periodic sets meet or a free surface exists. The interfaces are numbered starting from the top most free surface down to the bottom free surface. The system shown in Fig. 1 has four bi-periodic sets and five interfaces and the *state* of the system at any coordinate location consists of the temperature and flux.

### 2.2. Governing equations

The problem considered here is axisymmetric in nature and the governing equation for a single layer, in cylindrical coordinates, is given by:

$$\frac{\partial^2 T}{\partial r^2}+\frac{1}{r}\frac{\partial T}{\partial r}+\frac{\partial^2 T}{\partial z^2}=\frac{1}{\alpha}\frac{\partial T}{\partial t} \tag{1}$$

where $\alpha=\kappa/(\rho C_p)$, $\kappa$ is the conductivity, $\rho C_p$ is the heat capacity and $\alpha$ is the diffusivity of the layer. The temperature $T(r, z, t)$ is a function of radial and axial coordinates, $r$ and $z$, and of time $t$ and zero initial condition is assumed throughout the medium. The boundary conditions are given by:

$$\begin{aligned} &T(r,0,t)=T_T, \quad -k\frac{\partial T}{\partial z}(r,0,t)=F_T \\ &T(r,H,t)=T_B, \quad -k\frac{\partial T}{\partial z}(r,H,t)=F_B \end{aligned} \tag{2}$$

where $F$ is the flux, $H$ is the thickness of the layer and the subscripts 'T' and 'B' stand for the top and bottom surfaces of the layer, respectively. At this point, it is useful to introduce the scalings $\rho=r/H$, $\zeta=z/H$ and $\tau=t\alpha/H^2$ to reduce Eqs. (1) and (2) to the dimensionless form given by:

$$\frac{\partial^2 T}{\partial \rho^2}+\frac{1}{\rho}\frac{\partial T}{\partial \rho}+\frac{\partial^2 T}{\partial \zeta^2}=\frac{\partial T}{\partial \tau}$$

$$\begin{aligned} &T(\rho,0,\tau)=T_T, \quad -k\frac{\partial T}{\partial \zeta}(\rho,0,\tau)=HF_T \\ &T(\rho,1,\tau)=T_B, \quad -k\frac{\partial T}{\partial \zeta}(\rho,1,\tau)=HF_B \end{aligned} \tag{3}$$

Applying the Laplace transform with respect to time and a zero-order Hankel transform with respect to $\rho$ in Eq. (3) and incorporating the initial condition, the following ODE in the variable $\zeta$ is obtained:

$$\frac{d^2\bar{T}^0}{d\zeta^2}=(\mu^2+s)\bar{T}^0 \tag{4}$$

where $s$ and $\mu$ are the Laplace and Hankel transform variables, respectively. The overline indicates that Laplace transformation has been performed on the non-dimensional time variable $\tau$ and the superscript '0' indicates that a Hankel transform of order zero has been applied to the variable $\rho$. The solution to Eq. (4) is

$$\bar{T}^0=A\,e^{\beta\zeta}+B\,e^{-\beta\zeta} \tag{5}$$

where $\beta=\sqrt{\mu^2+s}$, and $A$ and $B$ are the constants of integration. Eq. (5) can be differentiated with respect to $\zeta$ to yield

$$\kappa\frac{\partial\bar{T}^0}{\partial\zeta}=\kappa\beta\,e^{\beta\zeta}A-\kappa\beta\,e^{-\beta\zeta}B \tag{6}$$

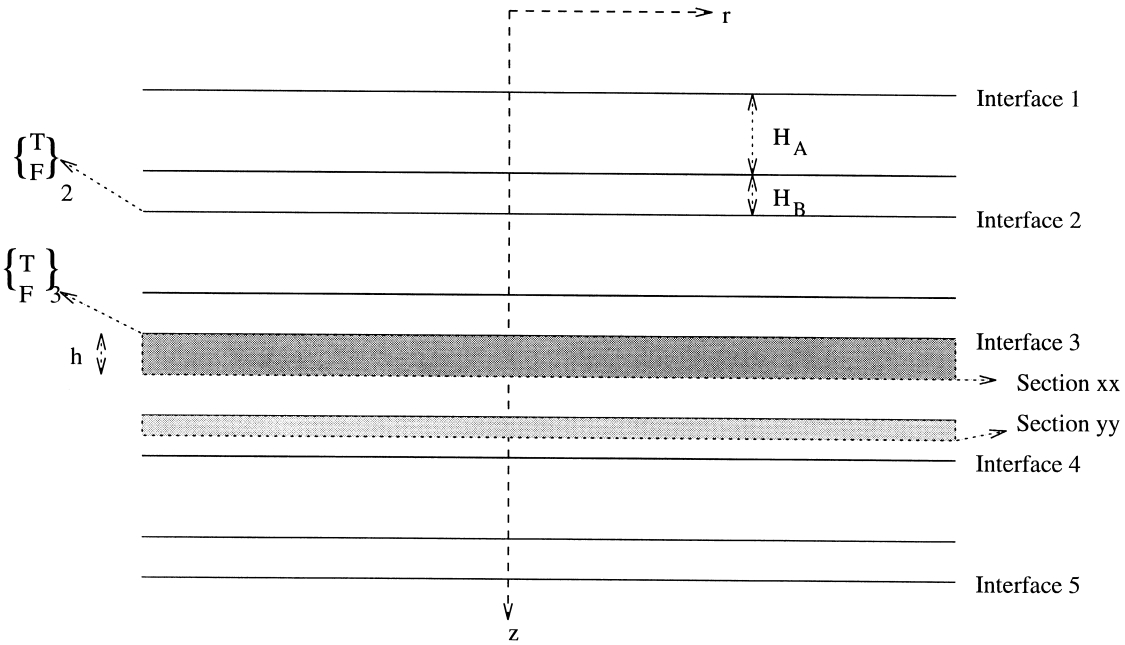


Fig. 1. A composite layered structure.

The boundary conditions in Eq. (3) are also transformed and used to eliminate the constants of integration in Eq. (6) and yield the relation:

$$\begin{Bmatrix} \bar{T}^0 \\ \bar{f}^0 \end{Bmatrix}_{\mathrm{B}} = \begin{bmatrix} \cosh\beta & \frac{\sinh\beta}{\beta}\frac{H_{\mathrm{A}}}{\kappa_{\mathrm{A}}} \\ \beta\frac{\kappa_{\mathrm{A}}}{H_{\mathrm{A}}}\sinh\beta & \cosh\beta \end{bmatrix} \begin{Bmatrix} \bar{T}^0 \\ \bar{f}^0 \end{Bmatrix}_{\mathrm{T}} = [T_{\mathrm{layer}}] \begin{Bmatrix} \bar{T}^0 \\ \bar{f}^0 \end{Bmatrix}_{\mathrm{T}} \tag{7}$$

where $\bar{f}^0 = -\bar{F}^0/H$ is the same as the negative of the transformed flux in the actual unscaled coordinate. The subscripts 'B' and 'T' refer to the bottom and top of the layer, respectively. The advantage of such a matrix representation will become evident when two layers are brought in contact in the transfer matrix formulation for the bi-periodic set. The matrix $[T_{\mathrm{layer}}]$ is the transfer matrix relating the states on the top and bottom surfaces of a single layer. Next, a similar transfer matrix for a bi-periodic set is derived.

### 2.3. The transfer matrix of a bi-periodic set

The bi-periodic set is composed of layers A and B, and the transfer matrix for these layers are used to construct the transfer matrix of the set. The transfer matrix of Layer A, termed $[T_{\mathrm{A}}]$, is obtained by directly substituting the thermal and geometrical properties of the layer in the matrix $[T_{\mathrm{layer}}]$ (see Eq. (7))

$$\begin{Bmatrix} \bar{T}^0_{\mathrm{A}} \\ \bar{f}^0_{\mathrm{A}} \end{Bmatrix}_{\mathrm{B}} = \begin{bmatrix} \cosh\beta & \frac{\sinh\beta}{\beta}\frac{H_{\mathrm{A}}}{\kappa_{\mathrm{A}}} \\ \beta\frac{\kappa_{\mathrm{A}}}{H_{\mathrm{A}}}\sinh\beta & \cosh\beta \end{bmatrix} \begin{Bmatrix} \bar{T}^0_{\mathrm{A}} \\ \bar{f}^0_{\mathrm{A}} \end{Bmatrix}_{\mathrm{T}} = [T_{\mathrm{A}}] \begin{Bmatrix} \bar{T}^0_{\mathrm{A}} \\ \bar{f}^0_{\mathrm{A}} \end{Bmatrix}_{\mathrm{T}} \tag{8}$$

where the inner subscript 'A' is used to indicate that the Layer A is considered. While deriving the transfer matrix for Layer B, care should be taken to maintain the consistency in the Hankel and Laplace transform variables. Now, the scalings $\rho = r/H_{\mathrm{A}}$, $\zeta = z/H_{\mathrm{B}}$ and $\tau = t\alpha_{\mathrm{A}}/H_{\mathrm{A}}^2$ are applied to the governing equations as was done in the derivation of $[T_{\mathrm{layer}}]$ and the transfer matrix for Layer B is obtained as:

$$\begin{Bmatrix} \bar{T}^0_{\mathrm{B}} \\ \bar{f}^0_{\mathrm{B}} \end{Bmatrix}_{\mathrm{B}} = \begin{bmatrix} \cosh\gamma & \frac{\sinh\beta}{\gamma}\frac{H_{\mathrm{B}}}{\kappa_{\mathrm{B}}} \\ \gamma\frac{\kappa_{\mathrm{B}}}{H_{\mathrm{B}}}\sinh\gamma & \cosh\gamma \end{bmatrix} \begin{Bmatrix} \bar{T}^0_{\mathrm{B}} \\ \bar{f}^0_{\mathrm{B}} \end{Bmatrix}_{\mathrm{T}} = [T_{\mathrm{B}}] \begin{Bmatrix} \bar{T}^0_{\mathrm{B}} \\ \bar{f}^0_{\mathrm{B}} \end{Bmatrix}_{\mathrm{T}} \tag{9}$$

where the inner subscripts define the layer, whereas the outer subscripts denote the top 'T' or bottom 'B' of each layer.

The transfer matrix of a bi-periodic set can be derived from $[T_{\mathrm{A}}]$ and $[T_{\mathrm{B}}]$ by imposing the conditions of continuity in flux and temperature at the interface where the layers meet. The conditions are $(\bar{T}^0_{\mathrm{A}})_{\mathrm{B}} = (\bar{T}^0_{\mathrm{B}})_{\mathrm{T}}$ and $(\bar{f}^0_{\mathrm{A}})_{\mathrm{B}} = (\bar{f}^0_{\mathrm{B}})_{\mathrm{T}}$, and yield the transfer matrix for a bi-periodic set.

$$[T_{\mathrm{set}}] = \begin{bmatrix} \cosh\gamma\cosh\beta + \frac{\tau\beta}{\gamma}\sinh\beta\sinh\gamma \\ \frac{1}{C_{\mathrm{B}}}\left[\frac{\cosh\gamma\sinh\beta}{\beta\tau} + \frac{\sinh\gamma\cosh\beta}{\gamma}\right] \\ C_{\mathrm{B}}\left[\beta\tau\sinh\beta\cosh\gamma + \gamma\sinh\gamma\cosh\beta\right] \\ \cosh\gamma\cosh\beta + \frac{\gamma}{\beta\tau}\sinh\gamma\sinh\beta \end{bmatrix}$$

The constants $\tau^* = C_{\mathrm{A}}/C_{\mathrm{B}}$ and $\eta = \alpha_{\mathrm{A}}/\alpha_{\mathrm{B}}$ are referred to as the *thermal impedance* and *scattering constant*, respectively. By dropping subscripts, the matrix equations relating the three states at the top and bottom of a bi-periodic set can now be expressed as

$$\left\{ \bar{T}^0 \quad \bar{f}^0 \right\}^{\mathrm{T}}_{i+1} = [T_{\mathrm{set}}] \left\{ \bar{T}^0 \quad \bar{f}^0 \right\}^{\mathrm{T}}_{i} \tag{10}$$

where the subscript '$i$' refers to the state at the top of the $i$th bi-periodic set and the superscript 'T' denotes the transpose.

### 2.4. Obtaining the states of a composite system at the interfaces

As mentioned previously, a layered composite system, in general, consists of $N$ bi-periodic sets as shown in Fig. 1. The states at the first and the last interfaces can be obtained from Eq. (10) by successive multiplications.

$$\left\{ \bar{T}^0_{N+1} \quad \bar{f}^0_{N+1} \right\}^{\mathrm{T}} = [T_{\mathrm{set}}]^N = \left\{ \bar{T}^0_1 \bar{f}^0_1 \right\}^{\mathrm{T}} \tag{11}$$

If any two of the four quantities $\bar{T}^0_1$, $\bar{T}^0_{N+1}$, $\bar{f}^0_1$ and $\bar{f}^0_{N+1}$ are known, the other two can be solved for. Here, it is assumed that the temperatures at the first and the last interfaces are prescribed. The variables $\bar{f}^0_i$ can then be solved in terms of the temperatures as follows:

$$\bar{f}^0_1 = \frac{\bar{T}^0_{N+1} - \alpha_{11}\bar{T}^0_1}{\alpha_{12}}$$

$$\bar{f}^0_{N+1} = \alpha_{21}\bar{T}^0_1 + \frac{\alpha_{22}}{\alpha_{12}}\left(\bar{T}^0_{N+1} - \alpha_{11}\bar{T}^0_1\right) \tag{12}$$

where $\alpha_{ij}$s are the entries of the $2 \times 2$ matrix $[T_{\mathrm{set}}]^N$.

Once the states at the top and bottom free surfaces of the system are known, the states at the internal interfaces can be obtained using Eq. (10). This method is called the *Method of Direct Multiplication*. These successive multiplications introduce severe errors in the

computation. This is because of the fact that the matrix $T_{set}$ contains hyperbolic sines and cosines whose arguments can take large values. As a result, the entries of $[T_{set}]$ can become large and the entries of $[T_{set}]^N$ can exceed computer precision. Severe truncations and round-offs occur and this situation is termed as *exponential dichotomy* [14].

An alternate scheme based on the Direct Global Transfer Matrix method developed in [15] is presented below. As will be shown in numerical examples later, this method virtually eliminates the problem of exponential dichotomy. In this approach, termed as DGTM method, instead of solving for the temperature and flux at different interfaces successively, a single state vector $\{\underline{s}\}$ of the unknown quantities is formed and is solved in a single step. The boundary conditions are assumed to be specified temperatures at the first and last interfaces of the system. One defines at this point the following vectors:

$$\{\underline{s}\} = \{f_1 \quad T_2 \quad f_2 \quad T_3 \cdots \quad T_N \quad F_N \quad F_{N+1}\}$$

$$\{\underline{f}\} = \{T_1 \quad T_1 \quad 0 \quad 0 \cdots 0 \quad T_{N+1} \quad 0\}$$

where $\{\underline{s}\}$ and $\{\underline{f}\}$ denote the unknown vector of internal states, and the known applied temperature "force" vector, respectively. Now, relating the unknown and known quantities for each periodic set separately, and combining them together into a single matrix equation, a new global transfer matrix is termed in the following form:

$$[C]\{\underline{s}\} = \{\underline{f}\} \tag{13}$$

where $[C]$ is given by

$$[C] = \begin{bmatrix} -t_{12}/t_{11} & 1/t_{11} & 0 & 0 & 0 & 0 & 0 & \cdots & 0 & 0 & 0 \\ -t_{22}/t_{21} & 0 & 1/t_{21} & 0 & 0 & 0 & 0 & \cdots & 0 & 0 & 0 \\ 0 & -t_{11} & -t_{12} & 1 & 0 & 0 & 0 & \cdots & 0 & 0 & 0 \\ 0 & -t_{21} & -t_{22} & 0 & 1 & 0 & 0 & \cdots & 0 & 0 & 0 \\ 0 & 0 & 0 & -t_{11} & -t_{12} & 1 & 0 & \cdots & 0 & 0 & 0 \\ 0 & 0 & 0 & -t_{21} & -t_{22} & 0 & 1 & \cdots & 0 & 0 & 0 \\ \vdots & \vdots & \vdots & \vdots & \vdots & \vdots & \vdots & \ddots & \vdots & \vdots & \vdots \\ 0 & 0 & 0 & 0 & 0 & 0 & 0 & \cdots & t_{11} & t_{12} & 0 \\ 0 & 0 & 0 & 0 & 0 & 0 & 0 & \cdots & t_{21} & t_{22} & -1 \end{bmatrix} \tag{14}$$

and $t_{ij}$s are the entries of the $2 \times 2$ matrix $[T_{set}]$.

Once the vector $f$ and the matrix $[C]$ have been computed, the unknown state vector $s$ can be obtained by a single matrix inversion:

$$\{\underline{s}\} = [C]^{-1}\{\underline{f}\} \tag{15}$$

The dimension of the matrix $[C]$ is $(N \times N)$, and if many bi-periodic layers are considered, the matrix inversion (Eq. (15)) becomes computationally challenging. However, the accuracy of the resulting vector of transformed states, $\{\underline{s}\}$, is guaranteed.

### 2.5. Obtaining the states of a composite system inside the layers

The methods discussed in earlier sections can be used to compute the transformed temperatures and fluxes at different interfaces of the composite system. It is essential to know the distribution of temperature in the composite structure as a whole. Hence, it is desired to compute the states inside the layers and not just at interfaces between layers. Once the states of the system at the interfaces have been computed, the computation of the transformed temperature and flux inside the layers is a straight forward task, at any axial distance for a given value of $s$ and $\mu$ (the Laplace and Hankel variables, respectively).

Considering the $m$th bi-periodic set, if the states are to be computed at the sections xx (see Fig. 1), the following arguments hold. The temperature and flux at the $m$th interface $\{\bar{T}^0_m \quad \bar{f}^0_m\}^{\mathrm{T}}$ have already been solved for. A fictitious layer, Layer C, having the thermal properties of Layer A and of thickness $h$ is assumed to exist (see Fig. 1). A transfer matrix $[T_h]$ can be derived for this layer in a manner similar to the derivation of the transfer matrix for Layer B. The matrix $[T_h]$, which gives the states at section xx, is given by:

$$\begin{Bmatrix} \bar{T}^0_h \\ \bar{f}^0_h \end{Bmatrix} = [T_h] \begin{Bmatrix} \bar{T}^0_m \\ \bar{f}^0_m \end{Bmatrix} = \begin{bmatrix} \cosh\gamma & \frac{\sinh\beta}{\gamma}\frac{h}{\kappa_A} \\ \gamma\frac{\kappa_A}{h}\sinh\gamma & \cosh\gamma \end{bmatrix} \begin{Bmatrix} \bar{T}^0_m \\ \bar{f}^0_m \end{Bmatrix} \tag{16}$$

where $\gamma = (h\sqrt{\mu^2 + s})/H_A$. The state at a depth $h$ inside Layer $B$ of the $m$th bi-layered set is (section yy of Fig. 1), can be computed as:

$$\begin{Bmatrix} \bar{T}^0_h \\ \bar{f}^0_h \end{Bmatrix} = [T'_h] \begin{Bmatrix} \bar{T}^0_{\text{inter}} \\ \bar{f}^0_{\text{inter}} \end{Bmatrix}$$

$$= \begin{bmatrix} \cosh\gamma & \frac{\sinh\beta}{\gamma}\frac{h}{\kappa_B} \\ \gamma\frac{\kappa_B}{h}\sinh\gamma & \cosh\gamma \end{bmatrix} [T_A] \begin{Bmatrix} \bar{T}^0_m \\ \bar{f}^0_m \end{Bmatrix}$$

$$= [T_h] \begin{Bmatrix} \bar{T}^0_m \\ \bar{f}^0_m \end{Bmatrix} \tag{17}$$

where $\gamma = (h\sqrt{\mu^2 + s\alpha_A/\alpha_B})/H_A$.

## 3. Transient responses of temperature and flux in the composite medium

In earlier sections, it was shown how the double-transformed temperatures and fluxes are computed free of numerical instabilities. In order to obtain them in the physical domain, the states previously computed have to be numerically inverted. To this end, a double integral inversion needs to be performed. Let the transformed temperature or flux at any location $\zeta$ of the layered medium be represented as $\bar{\psi}^0(\mu, \zeta, \omega)$, where $s = j\omega$ and $\mu$ are the Laplace and Hankel variables, respectively, and $\omega$ denotes frequency. The response in the physical domain is then expressed by the following double inversion:

$$\psi(\rho, \zeta, \tau) = \int_0^\infty \mu J_0(\mu\rho) \int_{-\infty}^{\infty} e^{-j\omega\tau} \bar{\psi}^0(\mu, \zeta, \omega)\, d\omega\, d\mu \tag{18}$$

where $J_0$ is the Bessel function of order zero. The variable $\rho$ is the scaled radial distance at which the state $\psi$ is desired. The Laplace variable $s$ is replaced by $j\omega$ to make the computational task easier, as standard Fast Fourier Transform (FFT) routines can be used to evaluate the inner integral in Eq. (18). For computational purpose, the limits of integration has to be finite.

The kernel of the integral in Eq. (18) dies out at finite values of and, and hence, the time response can be approximately expressed with the finite integral,

$$\psi(\rho, \zeta, \tau) = \int_0^{\mu_f} \mu J_0(\mu\rho) \int_{-\omega_f}^{\omega_f} e^{-j\omega\tau} \bar{\psi}^0(\mu, \zeta, \omega)\, d\omega\, d\mu \tag{19}$$

where $\omega_f$ and $\mu_f$ are the values of $\omega$ and $\mu$ at which the kernel's contribution is small. The integrals in the approximation in Eq. (19) can be evaluated numerically to yield the transient temperatures and fluxes at the desired locations.

The following is the typical procedure of computing the time responses of the temperatures and fluxes. The boundary conditions $T_1(r, t)$ and $T_5(r, t)$ have to be converted into the scaled coordinate system $(\rho, \tau)$. Then double integral transformations have to be applied and the quantities $\bar{T}^0_1(\mu, \omega)$ and $\bar{T}^0_5(\mu, \omega)$ have to be computed at discrete values of $\mu$ and $\omega$. Then the matrix $[T_{\text{set}}]$ is evaluated at these $(\mu, \omega)$ combinations and stored. Using $\bar{T}^0_1(\mu, \omega)$, $\bar{T}^0_5(\mu, \omega)$ and $[T_{\text{set}}]$, the other unknown temperatures and fluxes at the various interfaces are computed using the DGTM method and stored in memory. When a state $\bar{\psi}^0(\mu, \zeta, \omega)$ is desired inside the layers, it can be computed using the methods mentioned earlier and they are also stored. The time response computation is done in two steps. First, a Inverse Fast Fourier Transform (IFFT) is applied to the variable $\bar{\psi}^0(\mu, \zeta, \omega)$ for each of the discrete values of $\mu$ to obtain $\psi^0(\mu, \zeta, \tau)$ which shall be referred to as *time modes*. Then the inverse Hankel transformation is computed at a given $\rho$ value using a seven-point quadrature integration scheme which goes by the name DAVINT. This is more than sufficient because the time modes are not oscillatory in nature. The key in performing the inversions is to select the proper limits of integration. The only way to select these limits is to look at the values of the kernel for various $(\mu, \omega)$ values and carefully fix the limits at a point where the kernels contribution is negligible.

In the next section, an example is considered to illustrate the method and the numerical problems that may be encountered. Also, a comparison of the DGTM and the Direct Multiplication Method is provided.

## 4. Numerical simulations

For the numerical simulations considered in this paper, we look at two systems named Systems I and II. System I consists of eight layers of $Al_2O_3$, while System II consists of eight layers with layers of $Al_2O_3$ and $ZrO_2$ alternating. The thickness of each layer is 1 mm. The properties of the materials are; $Al_2O_3$: $\kappa = 20.934$ W/cm/°C, $\rho C_p = 1.779 \times 10^6$ W s/(K m$^3$), $ZrO_2$: $\kappa = 4.1868$ W/cm/°C, $\rho C_p = 8.303 \times 10^5$ W s/(K m$^3$). For these parameters, the values of $(\tau^*, \eta)$ are (1, 1) for System I and (5, 2.33) for System II.

A simulation is performed on System II to illustrate the occurrence of exponential dichotomy and to obtain the transient responses. The specified temperature distributions on Interfaces 1 and 5 are shown in Fig. 2. The goal is to find the transient temperature ($T_3$) and flux ($f_3$) at the third interface. Both the DGTM and the Direct Multiplication methods can be used. In

order to determine the limits of integration of the double integral inverse transformation in Eq. (19), the kernel has to be evaluated at various $\mu$ and $\omega$ values. This is where the problem arises. If Direct Multiplication is used, exponential dichotomy sets in for values of $\mu$ greater than 5. In Figs. 3 and 4, the onset of exponential dichotomy while using the Direct Multiplication method is illustrated. The DGTM method for the same setting is free of numerical errors. The variables $\bar{T}_3^0$ and $\bar{f}_3^0$ are evaluated for a $\mu$ range of 0.0001–15 and $\omega$ range of 0–15. Based on the simulations, the limits of integration were set to $\mu_f = 5$ and $\omega_f = 5$. The time mode plots and the transient response of the temperature and flux at the third interface are shown in Fig. 5. As can be seen in the figures, the kernel for the Hankel Inversion (Fig. 5(b) and (d)) die out at $\mu = 0.9$ itself. At that value of $\mu$, the Direct Multiplication Method is stable.

Referring to Fig. 5(c), it can be noted that to begin with the flux (note that $f$ is the negative of the actual flux) is positive, meaning that heat is transferred from the fifth to the third interface. This is obvious because the temperature at the fifth interface is higher. At 200 s, steady state is reached. Then at 500 s when the thermal loading is removed, heat transfer occurs rapidly from the third to the fifth interface, and a reversal of the flux occurs.

Now, for the specified temperatures on the top and bottom surfaces as shown in Fig. 6, numerical simulations are performed on Systems I and II. The tem-

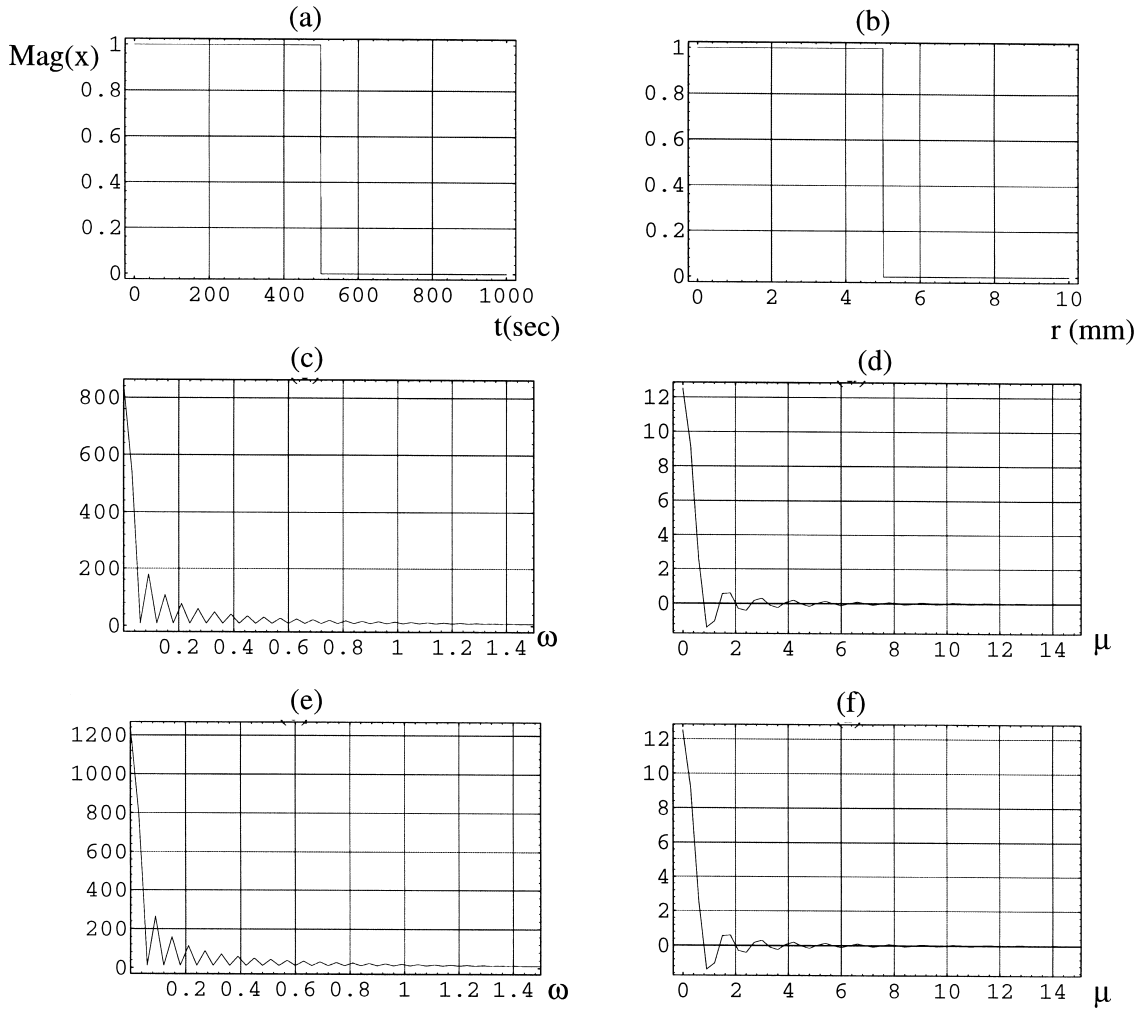


Fig. 2. (a) The time dependence of $T_1$ and $T_5$, the temperatures at the first and last interface. Mag = 1700 for $T_1$ and 2500 for $T_5$, (b) radial dependence of $T_1$ and $T_5$, (c) FFT of the time component of $T_1$, (d) Hankel transform of the radial component of $T_1$, (e) FFT of the time component of $T_5$, (f) Hankel transform of the radial component of $T_5$.

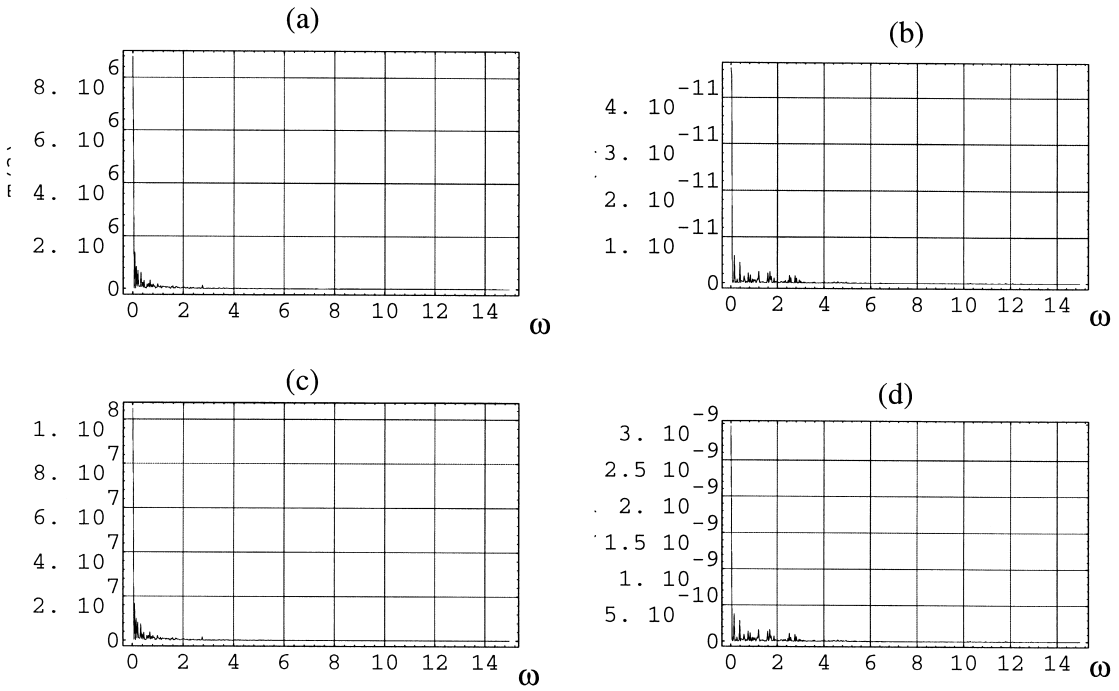


Fig. 3. (a) Transformed temperature $\bar{T}_3^0$ vs. $\omega$ at $\mu = 12$ using direct multiplication, (b) $\bar{T}_3^0$ at $\mu = 12$ using DGTM method, (c) transformed flux $\bar{f}_3^0$ at $\mu = 12$ using direct multiplication, (d) $\bar{f}_3^0$ at $\mu = 12$ using DGTM method.

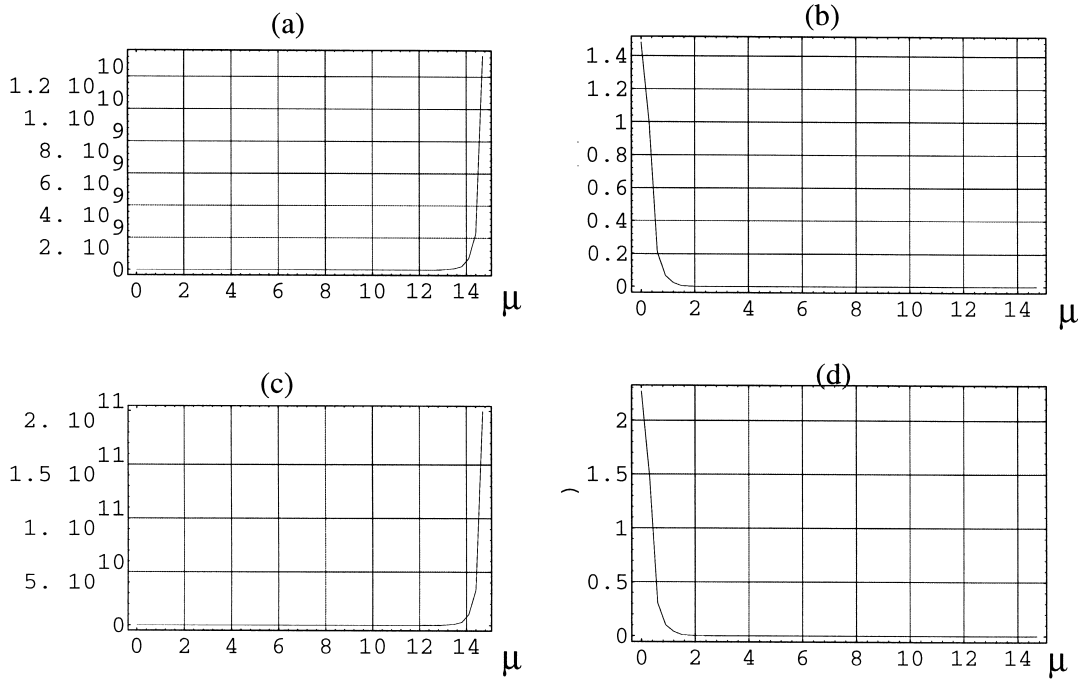


Fig. 4. (a) Transformed temperature $\bar{T}_3^0$ vs. $\mu$ at $\omega = 1.5$ using direct multiplication, (b) $\bar{T}_3^0$ at $\omega = 1.5$ using DGTM method, (c) transformed flux $\bar{f}_3^0$ at $\omega = 1.5$ using direct multiplication, (d) $\bar{f}_3^0$ at $\omega = 1.5$ using DGTM method.

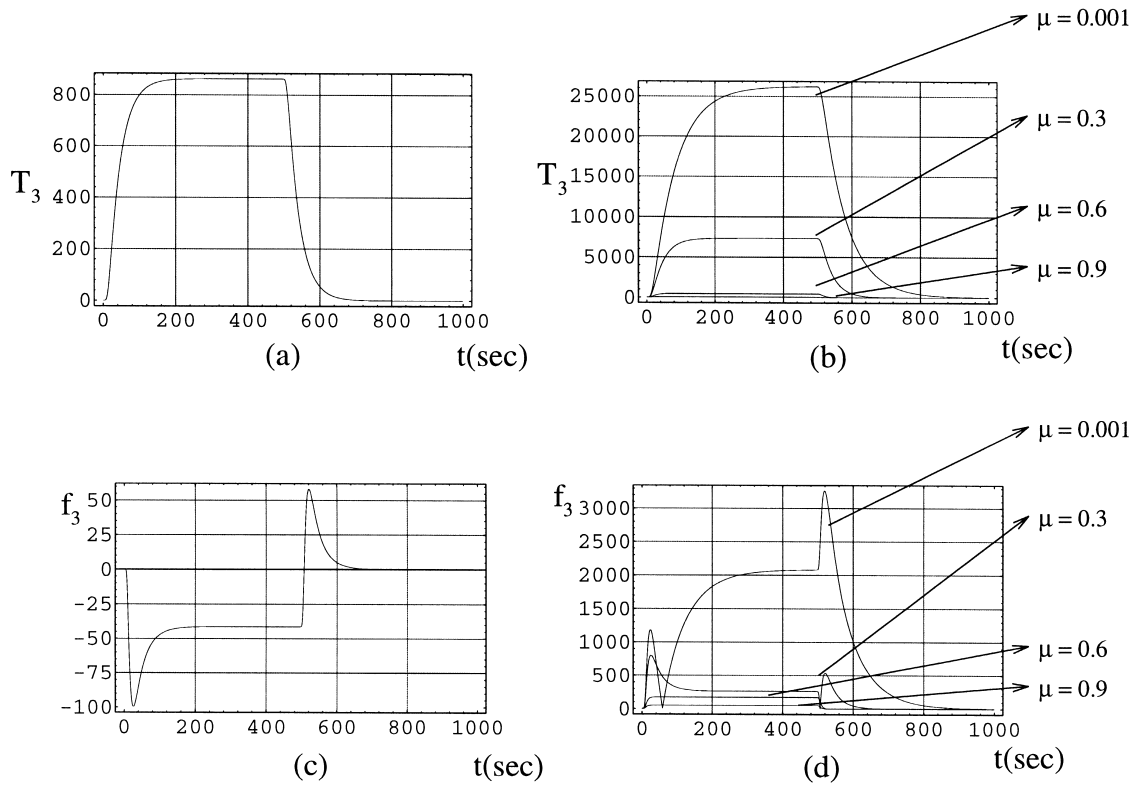


Fig. 5. (a) Transient response $T_3(t)$ at $r = 0$, (b) time modes of $T_3(t)$ vs. $t$ for $\mu$ values of 0.001, 0.3, 0.6, 0.9, (c) transient response $f_3(t)$ at $r = 0$, (d) time modes of $f_3(t)$ vs. $t$ for values of 0.001, 0.3, 0.6, 0.9.

perature distribution contours at various time instances are shown in Figs. 7 and 8. The temperature distribution plots of Systems I and II are given for the same range, for the sake of comparison. In order to obtain these plots, the variables were computed for the following range of variables. A $\omega$ range of 0–5 with 100 points and a $\mu$ range of 0.0001–5 with 50 points are considered. Also, the temperatures are computed for a $r$ range of −5–5 mm with 20 points and at $z$ locations at intervals of 0.1 mm.

It is evident from Figs. 7 and 8 that for System II, the heat diffusion from the upper to the lower surface is smaller than in System I. The heat is dissipated more freely in the radial direction. As a result, high

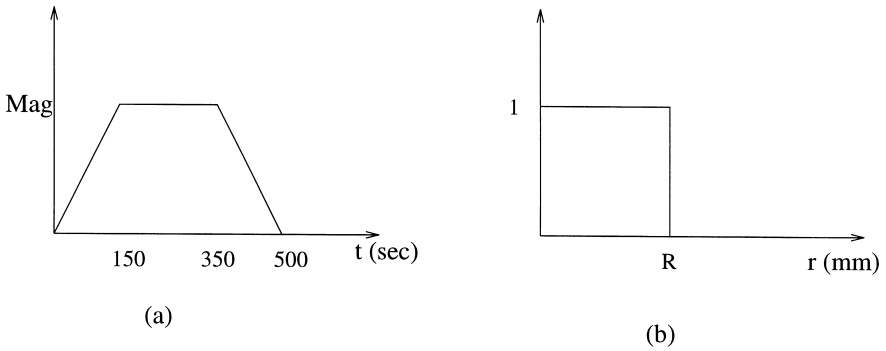


Fig. 6. The time dependence (a), and the radial dependence (b) of the temperature specified temperatures $T_1$ and $T_5$. Mag = $2700F$ and $R = 5$ for $T_1$ and Mag = $1700F$ and $R = 25$ for $T_5$.

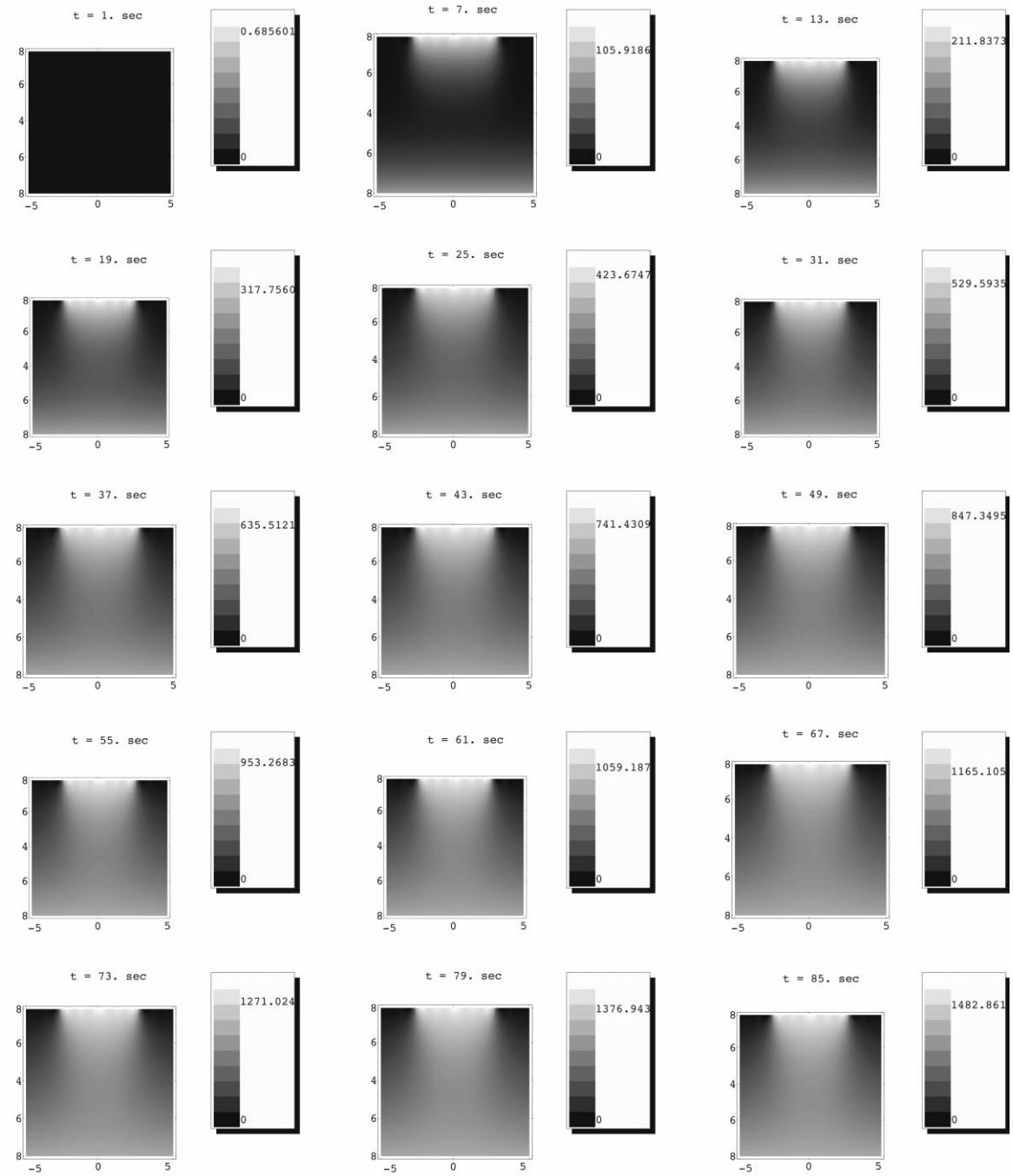


Fig. 7. Temperature contour plots of System I at $t = i\Delta t + 1$, $\Delta t = 6$ s, $i = 0, 1, \ldots, 14$.

temperatures are localized to the boundary layers of the system. This is due to the presence of weakly conducting layers sandwiched in between the strongly conducting layers. This lack of heat diffusion in the system with layers of different thermal conductivity can be used in the design of thermal coatings used for thermal protection of turbine blades. Similar localization phenomena of stress waves in layered media were reported by Cetinkaya and co-workers [7–11]. It was shown that when the layers of the system possess large differences in mechanical impedances, the axial wave transmission is impeded and energy localization

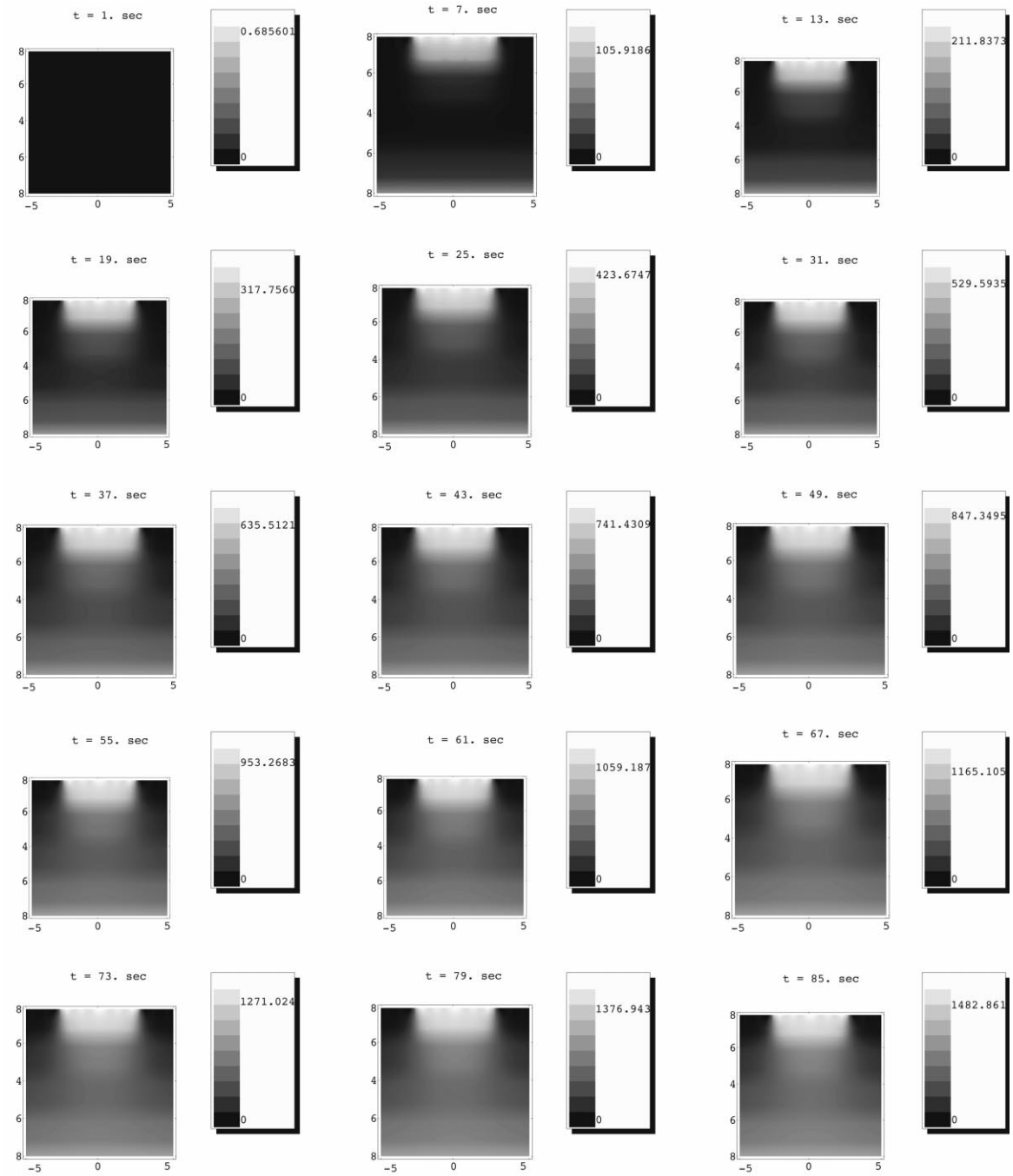


Fig. 8. Temperature contour plots of System II at $t = i\Delta t + 1$, $\Delta t = 6$ s, $i = 0, 1, \ldots, 14$.

in certain layers occur. In the above works obtaining the stresses were computationally involved, because in the wave propagation context, the time modes were highly oscillatory for high wave numbers ($\mu$). But in the current problem, this was not an issue, as the time modes for high $\mu$ values are smooth.

## 5. Discussion

We now provide some remarks regarding the technical details and the limitations of the described computational methodology. These remarks are necessary in order to apply correctly the double integral numerical

technique outlined in this work and deprive it of numerical instabilities.

It was mentioned earlier that if any two quantities (temperature, flux) are prescribed, then the outlined method can be used to yield the temperatures at any desired location. But due to the parabolic nature of the problem, it is essential that the variables should be bounded. As an example, it is incorrect to prescribe the temperature and the flux at the first interface and try to solve for the states elsewhere. This is because of the fact that the temperature and flux at the last interface is not bounded externally and there could be many solutions to the Boundary Value Problem; in that case, numerical instabilities will invariably aid in creating unrealistic solutions at the last interface. However, the temperature at the first interface and the flux at the last interface can be prescribed or vice versa.

In Ref. [12], it is noted that the transfer matrix method by direct multiplication can be applied to an unlimited number of layers. This is, however, true only when the parameter $\tau^*$ is very close to unity. When $\tau^*$ is away from unity, exponential dichotomy sets in even when a few layers are considered. In this case, the DGTM method can be used. But the trade off is the computational time. But relatively speaking, the computational time is not as high as in the wave propagation context [11], where the time modes had to be computed for a very high $\mu$ values, over a fine grid, and were also highly oscillatory in nature. In the heat diffusion problem, the time modes are not oscillatory, and hence, the $(\omega, \rho)$ grid on which the temperatures are computed need not be fine. Hence, computationally, the heat diffusion problem is less challenging than the corresponding wave propagation problem. The choice of the DGTM method or Direct Multiplication Method depends on the parameter of the system and computational time limits.

The indefinite integral in Eq. (18) is replaced by the definite integral of Eq. (19) under the assumption that the kernel dies out at high values of $\mu$ and $\omega$. But also the problem of exponential dichotomy sets in, wherein severe numerical errors are introduced in the computation of the matrix $[T_{\text{set}}]$ because of exponential terms involving $\mu$. The use of the DGTM formulation against the direct multiplication method delays the onset of exponential dichotomy to a great extent. It is observed that at some critical value of $\mu$, termed $\mu_{\text{cr}}$, numerical errors start to set in for the Direct Multiplication Method. In the case of a system containing few bi-periodic layers, the value of $\mu_{\text{cr}}$ is higher near the region of applied boundary conditions. At regions away from where the boundary conditions are applied, the value of $\mu_{\text{cr}}$ is much lower. But the kernel of the integral dies out at a value of $\mu$ lesser than $\mu_{\text{cr}}$. Hence, this value of $\mu$ is set as the upper limit of integration of the Hankel Inversion Integral. It would be erroneous to evaluate the kernel beyond this value of $\mu$, for the need of improved accuracy, as unwarranted numerical errors may set back the computations.

The errors in the Direct Multiplication Method can be reduced to a certain extent as follows. If the state at the fourth interface in Fig. 1 is to be computed, it can be obtained by means of successive multiplications as $\{\bar{T}_4^0 \quad \bar{f}_4^0\}^{\text{T}} = [T_{\text{set}}]^3\{\bar{T}_1^0 \quad \bar{f}_1^0\}^{\text{T}}$. We can alternately compute the state vector as $\{\bar{T}_4^0 \quad \bar{f}_4^0\}^{\text{T}} = [T_{\text{set}}]^{-1} \times \{\bar{T}_5^0 \quad \bar{f}_5^0\}^{\text{T}}$. The latter would help in reducing numerical instabilities in this method.

We note that the formulation and the results given above were only for specified temperature or flux on the top and bottom surface of the system. The same method can also be applied to systems with other kinds of mixed boundary conditions. For example, a convective boundary condition can be prescribed or there could be convective layers sandwiched between layers. Suppose there is a convective stream with a free stream temperature $T_\infty$ on the first interface. A transfer matrix can be derived relating $T_\infty, f_\infty$ and $T_1$, $f_1$, and the rest of the method can be applied as described above. Radiative boundary conditions can also be approximated as convective boundary conditions and solutions can be obtained iteratively.

In the numerical simulations of the previous section, the matrix $[T_{\text{set}}]$ is not evaluated at $\mu = 0$ but at a small initial value. This is because of the fact that the matrix $[T_{\text{set}}]$ is singular to computer precision at $\mu = 0$ and $\omega = 0$. Alternatively, the matrix can be evaluated starting at small $\omega$ and starting from $\mu = 0$. But this will affect the inverse Fast Fourier Transform computations.

Finally, we note that in the numerical simulations, the state variables were evaluated on a fine grid of $\mu$ values. This is actually unnecessary. The time modes of the temperatures and fluxes (for example, see Fig. 5(b) and (d)) vary very smoothly with $\mu$, and in addition, the use of a seven point integration scheme, can interpolate very accurately the kernel for the evaluation of inverse Hankel integral.

## Acknowledgements

All simulations have been performed on the Silicon Graphics Power Challenge Array at the National Center for Supercomputing Applications (NCSA) in the University of Illinois at Urbana-Champaign. NCSAs support in the form of supercomputer time allocation is greatly appreciated. This work was supported in part by a grant from EPRI (Dr. Martin Wildberger is the grant monitor), NSF Young Investigator award CMS-9457750 (Dr. Devendra Garg is the grant monitor), and the Department of Mechan-

ical and Industrial Engineering of the University of Illinois at Urbana-Champaign. This support is gratefully acknowledged.

## References

[1] J. Baker-Jarvis, R. Inguva, Heat conduction in layered composite materials, Journal of Applied Physics 57 (1985) 1569–1573.
[2] J.K. Baumeister, T.D. Hammil, Hyperbolic heat-conduction equation — a solution for the semi-infinite body problem, Journal of Heat Transfer (1969) 543–548.
[3] M.N. Ozisik, B. Vick, Propagation and reflection of thermal waves in a finite medium, International Journal of Heat and Mass Transfer 27 (1984) 1845–1854.
[4] R. Yalamanchili, S.C. Chu, Transient two-dimensional heat transfer in composite media, Numerical Methods in Thermal Problems (1983) 54–64.
[5] Wu. Chih-Yang, Ou. Nai-Rui, Transient two-dimensional radiative and conductive heat transfer in a scattering medium, International Journal of Heat and Mass Transfer 37 (1994) 2675–2686.
[6] M. Bouzidi, P. Duhamel, Thermal diffusion in cyclic laminated composites: spectral properties and application to the homogenization, International Journal of Heat and Mass Transfer 36 (1993) 2715–2723.
[7] C. Cetinkaya, Axisymmetric stress wave propagation in weakly coupled layered structures: analytical and computational studies, Ph.D. Thesis, Department of Aeronautical and Astronautical Engineering, University of Illinois at Urbana-Champaign, 1995.
[8] A.F. Vakakis, C. Cetinkaya, M. El-Raheb, Axisymmetric elastic wave propagation in weakly coupled layered media of infinite radial extent, Journal of Sound and Vibration 182 (1995) 283–302.
[9] C. Cetinkaya, A.F. Vakakis, Transient axisymmetric stress wave propagation in weakly coupled layered structures, Journal of Sound and Vibration 194 (1996) 389–416.
[10] M. El-Raheb, A.F. Vakakis, C. Cetinkaya, Free and forced dynamics of a class of periodic elastic systems, Journal of Sound and Vibrations 172 (1994) 23–46.
[11] C. Cetinkaya, J. Brown, A.A.F. Mohammed, A.F. Vakakis, Near field transient axisymmetric waves in structures: effects of weak coupling, International Journal for Numerical Methods in Engineering 40 (1997) 1639–1665.
[12] P.H. Leturcq, J.M. Dorkel, F.E. Ratolojanahary, S. Tounsi, A two-port network formalism for 3D hear conduction analysis in multilayered media, International Journal of Heat and Mass Transfer 36 (1993) 2317–2326.
[13] M.N. Ozisik, Heat Conduction, 2nd ed., Wiley, New York, 1993.
[14] A.K. Mal, Wave propagation in layered composite laminates under periodic surface loads, Wave Motion 10 (1988) 257–266.
[15] H. Schmidt, F. Jensen, An efficient numerical solution technique for wave propagation in horizontally stratified ocean environments, SACLANTCEN Memorandum, SM-173, SACLANTCEN, 1984.